

(This is a sample cover image for this issue. The actual cover is not yet available at this time.)

This article appeared in a journal published by Elsevier. The attached copy is furnished to the author for internal non-commercial research and education use, including for instruction at the authors institution and sharing with colleagues.

Other uses, including reproduction and distribution, or selling or licensing copies, or posting to personal, institutional or third party websites are prohibited.

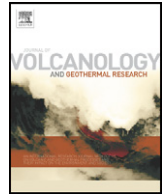
In most cases authors are permitted to post their version of the article (e.g. in Word or Tex form) to their personal website or institutional repository. Authors requiring further information regarding Elsevier's archiving and manuscript policies are encouraged to visit:

<http://www.elsevier.com/copyright>



Contents lists available at SciVerse ScienceDirect

Journal of Volcanology and Geothermal Research

journal homepage: www.elsevier.com/locate/jvolgeores

Diverse subaerial and sublacustrine hot spring settings of the Cerro Negro epithermal system (Jurassic, Deseado Massif), Patagonia, Argentina

Diego M. Guido ^{a,*}, Kathleen A. Campbell ^b^a CONICET and Facultad de Ciencias Naturales y Museo, Universidad Nacional de La Plata, Instituto de Recursos Minerales (INREMI), Calle 64 y 120, La Plata (1900), Argentina^b Geology, School of Environment, University of Auckland, Private Bag 92019, Auckland 1142, New Zealand

ARTICLE INFO

Article history:

Received 30 December 2011

Accepted 23 March 2012

Available online 31 March 2012

Keywords:

Deseado Massif

Patagonia

Jurassic hot springs

Travertine

Silicification

Subaerial

Sublacustrine

ABSTRACT

The Late Jurassic (~150 Ma) Cerro Negro volcanic–epithermal–geothermal system (~15 km² area), Deseado Massif, Patagonia, Argentina, includes two inferred volcanic emission centers characterized by rhyolitic domes linked along NW–SE regional faults that are associated with deeper level Au/Ag mineralization to the NW, and with shallow epithermal quartz veins and mainly travertine surface hot spring manifestations to the SE. Some travertines are silica-replaced, and siliceous and mixed silica–carbonate geothermal deposits also are found. Five hot spring-related facies associations were mapped in detail, which show morphological and textural similarities to Pleistocene–Recent geothermal deposits at Yellowstone National Park (U.S.A.), the Kenya Rift Valley, and elsewhere. They are interpreted to represent subaerial travertine fissure ridge/mound deposits (low-flow spring discharge) and apron terraces (high-flow spring discharge), as well as mixed silica–carbonate lake margin and shallow lake terrace vent-conduit tubes, stromatolitic mounds, and volcano-shaped cones. The nearly 200 mapped fossil vent-associated deposits at Cerro Negro are on a geographical and numerical scale comparable with subaerial and sublacustrine hydrothermal vents at Mammoth Hot Springs, and affiliated with Yellowstone Lake, respectively. Overall, the Cerro Negro geothermal system yields paleoenvironmentally significant textural details of variable quality, owing to both the differential preservation potential of particular subaerial versus subaqueous facies, as well as to the timing and extent of carbonate diagenesis and silica replacement of some deposits. For example, the western fault associated with the Eureka epithermal quartz vein facilitated early silicification of the travertine deposits in the SE volcanic emission center, thereby preserving high-quality, microbial macro- and micro-textures of this silica-replaced “pseudosinter.” Cerro Negro provides an opportunity to reconstruct paleogeographic, paleohydrologic and paleoenvironmental associations in a well-exposed, extensive and diverse fossil geothermal system. This Late Jurassic hydrothermal deposit will likely contribute to a better understanding of the impact of depositional and post-depositional history on the development and long-term preservation potential of Lagerstätte in epithermal settings and, more generally, in extreme environments of the geological record.

© 2012 Elsevier B.V. All rights reserved.

1. Introduction and regional setting

The Deseado Massif (Santa Cruz Province, southern Patagonia) is a 60,000 km² crustal block typified by extensive (>30,000 km²), Middle to Late Jurassic, bimodal volcanic and related rocks of the Bahía Laura Complex (BLC), including Chon Aike rhyolites intercalated with Bajo Pobre andesites, and reworked volcanoclastics of the La Matilde Formation (Fig. 1A; Echeveste et al., 2001; Guido, 2004; Guido et al., 2006). In broad terms, La Matilde strata, including fossil hot spring deposits, are found at the top of the sequence together with intermediate to silicic lava domes of the BLC, and accumulated in a mature (quiescent) phase of volcanism during the

Late Jurassic (Guido, 2004). Collectively these rocks are part of the Chon Aike Silicic Large Igneous Province (Argentinean Patagonia to Antarctica; Pankhurst et al., 1998), developed in a diffuse extensional back-arc setting associated with opening of the South Atlantic Ocean (cf. Richardson and Underhill, 2002).

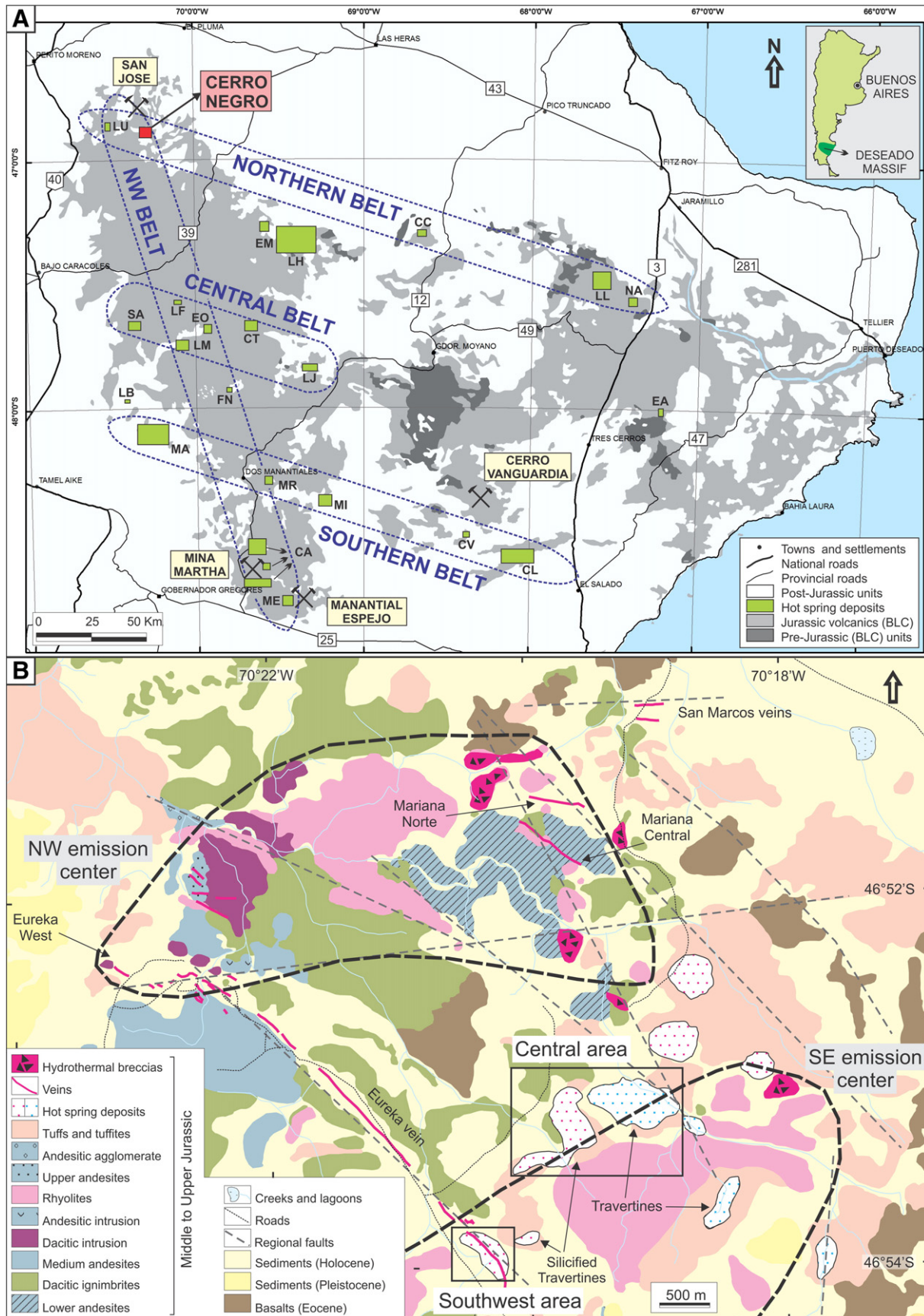
Over an ~30 m.y. interval in the Middle to Late Jurassic (ca. 178–151 Ma), extension, magmatism and a high thermal gradient produced BLC volcanism and related hydrothermal mineralization in the Deseado Massif, including economic gold- and silver-bearing, mainly low-sulfidation type epithermal quartz veins, and numerous hot spring occurrences (Fig. 1A; Guido and Schalamuk, 2003; Guido and Campbell, 2011). Four mines are currently in production and two, including Cerro Negro, are under construction. Based on measured and indicated resources, Cerro Negro, in particular, is set to become one of the largest gold producers in the Deseado Massif (5.3 Moz Au, 23.5 Moz Ag; Shatwell et al., 2011). The local and regional geologic contexts of the numerous geothermal and significant epithermal

* Corresponding author. Tel./fax: +54 221 4225648.

E-mail addresses: diegoguido@yahoo.com (D.M. Guido), ka.campbell@auckland.ac.nz (K.A. Campbell).

deposits of the Deseado Massif, and their alignment along major lineaments (confirmed by aeromagnetic data), together indicate structural control of Jurassic hydrothermal activity, with focus of

fluid upflow along the western and northern horst-like boundaries of the Massif itself (Guido and Schalamuk, 2003; Guido and Campbell, 2011).



Deseado Massif hot spring-related deposits comprise mostly travertines, some siliceous sinters, and geothermally related cherts, and are hosted in tuffs and reworked volcanoclastic sediments within fluviolacustrine settings over a 230×230 km area (Fig. 1A; Guido and Campbell, 2011). A regional hydrothermal silicification event overprinted many of these interbedded hot spring and volcanoclastic rocks during the Late Jurassic (Guido et al., 2002), indurating the deposits and thus generally increasing their long-term preservation potential. Nonetheless, depending on the local timing and extent of late stage mineralization with respect to depositional history, original textural and compositional details became obscured at a number of sites. On the other hand, for some deposits that experienced pervasive early silicification, hot spring-related facies of exceptional preservation also can be found (e.g., San Agustín Lagerstätten: Guido et al., 2010; Channing et al., 2011; García Massini et al., 2012).

The Jurassic Patagonian rocks subsequently were buried by Cretaceous and Cenozoic continental and marine passive margin successions (Giacosa et al., 2010), and then unearthed with minimal structural disturbance to expose intact, erosional windows into 23 mapped subaerial and/or sublacustrine geothermal systems (Guido and Campbell, 2011). At several locations, including Cerro Negro (Fig. 1B), both the fossil “plumbing” and paleosurface expressions of hydrothermal activity are evident (e.g., epithermal quartz veins, hydrothermal breccias, hot spring deposits), with diverse geothermal landscapes represented (Fig. 2). Such three-dimensional spatial associations of fossil hydrothermal deposits enable detailed paleogeographic, paleoenvironmental and paleohydrologic reconstructions (e.g., Guido and Campbell, 2009; Guido et al., 2010). They also provide glimpses into the inner workings of entire volcanic–geothermal–epithermal systems rarely possible in other older or younger continental hydrothermal settings elsewhere in the world.

The aim of this study is to evaluate in detail the geologic context and diverse facies associations of the hot spring-related deposits at Cerro Negro, for which only a few portions have received cursory descriptions (Guido et al., 2002; Lopez et al., 2003; Lopez, 2006). Five types of calcareous and siliceous surface hydrothermal manifestations are evident, which are similar to Pleistocene–Recent, geothermally affiliated deposits of Yellowstone National Park (Wyoming, U.S.A.), the Kenya Rift Valley, and elsewhere. These constitute subaerial travertine (1) fissure ridges/mounds and (2) apron terraces, and mixed silica–carbonate lake margin and shallow lake terrace deposits, including (3) vent-conduit tubes, (4) stromatolitic mounds, and (5) volcano-shaped cones. Overall, this fossil geothermal system yields textural details of variable quality, owing to both the differential preservation potential of particular subaerial versus subaqueous facies, as well as to the timing and extent of carbonate diagenesis and silica replacement in some deposits. Hence, Cerro Negro provides an opportunity to assess the impact of depositional and post-depositional history on microfacies and microbial fossil preservation, thereby yielding clues to the controls affecting development and long-term preservation potential of Lagerstätte in epithermal settings and, more generally, in extreme environments of the geological record.

2. Results

2.1. Geology of the Cerro Negro hydrothermal system

The area of study (Fig. 1B) is located in the northwestern corner of the ~26,500 ha Cerro Negro mining property (Shatwell et al.,

2011, Fig. 2, p. 17), a prolific mining project that is developing toward precious metal production. It comprises low sulfidation epithermal gold- and silver-bearing quartz vein deposits hosted by Upper Jurassic andesitic to rhyodacitic volcanic and/or intrusive rocks (Shatwell et al., 2011). Fig. 1B (modified from Lopez, 2006) shows the geologic context of the study area. The Middle to Upper Jurassic Bahía Laura Complex here is composed of a volcanic sequence of andesitic lava flows interbedded with dacitic ignimbrites, andesitic and dacitic subvolcanic intrusions, and rhyolitic lava flows. BLC volcanic rocks have been interpreted to be co-genetic, and three U/Pb dates from the central units of the sequence yielded a 159–156 m.y. age range (Lopez, 2006). The BLC is topped by extensive fluviolacustrine volcanoclastic deposits, which are the product of a quiet depositional setting within a waning and post-volcanism interval. During the last stages of BLC volcanism, and as a consequence of a high geothermal gradient, a large hydrothermal system (~15 km²) developed in the Cerro Negro area, generating shallow, low sulfidation veins and breccias, regional hydrothermal alteration, and surface hot spring manifestations (Lopez, 2006).

To the northwest and southeast of the geothermal deposits comprising the study area, two large ENE–WSW volcanic emission centers can be inferred, as evidenced by rhyolitic domes and intermediate porphyritic intrusions (Fig. 1B). They are linked by major regional faults that, in between the two centers, host the epithermal occurrences in this part of the Cerro Negro project. High-grade mineralized structures (Eureka West, San Marcos, Mariana Central and Mariana Norte; from Shatwell et al., 2011) are concentrated within the NW emission center, and on both sides of this feature. The Eureka vein is the best exposed low sulfidation vein at Cerro Negro, and it outcrops along a fault that links the two emission centers. Lopez (2006) studied the Eureka vein in detail and, based on its mineralogy and textures, he divided it into three sectors. The northwestern sector was interpreted as the deepest and the southeastern as the shallowest.

Fossil hot spring deposits outcrop toward the interpreted SE volcanic emission center, consistent with the inference of increasingly shallow paleodepth along the Eureka vein, and they form a ring-like shape around the rhyolitic dome in this part of the study area (Fig. 1B). They are mainly travertine deposits, are silicified toward the ENE and WSW limits of the SE emission center, and have remained calcareous in the central portion that is geographically associated with the rhyolitic dome. There are several exposures of hot spring-related deposits, but only some of them are preserved well enough to allow detailed analysis, and these are located in the Central and Southwest study areas delineated herein (Fig. 1B).

The Central study area (Fig. 2A) consists of two groups of hot spring-related outcrops, situated north of the largest exposure of the rhyolitic dome affiliated with the SE emission center. The hot spring deposits are oriented in an ENE–WSW direction, offset from one another by an inferred normal NW–SE fault, and set in lacustrine to fluvial reworked volcanoclastic material. The Southwest study area (Fig. 2B) comprises an elongated NW outcrop of silica-replaced travertine within lacustrine volcanoclastic deposits, which is situated at the top of the shallowest (southeastern) sector of the Eureka vein.

2.2. Cerro Negro hot spring-related facies associations

Five types of hot spring-related deposits occur in the Cerro Negro geothermal system (Fig. 2). Two are shown herein to be subaerial in origin, constituting travertine fissure ridge/mound (Fig. 3) and silica-

Fig. 1. (A) Generalized geological data for the Deseado Massif, including geographic position of the Massif in Argentina (inset), and location of the Cerro Negro study area. Green boxes highlight the other 22 mapped hot spring localities, aligned in four major belts. Abbreviations – LU: La Unión, CC: Cerro Contreras, LL: La Leona, NA: Cañadón Nahuel, EM: El Macanudo, LH: La Herradura, EA: El Águila, SA: San Agustín, LF: La Flora, LM: La Marcelina, EO: Esperanza Oeste, CT: Cerro Tornillo, LJ: La Josefina, FN: Flecha Negra, LB: La Bajada, MA: La Marciana, MR: La María, MI: Monte Illiria, CV: Cerro Vanguardia, CL: Claudia, CA: Cerro 1 Abril, ME: Manantial Espejo. (B) Geological map of the Cerro Negro geothermal–epithermal system, with interpreted volcanic emission centers (black thick dashed lines). Boxes indicate the Central and Southwest study areas, shown in more detail in Fig. 2. Panel A is modified from and defined by Guido and Campbell, 2011 and Panel B is modified from Lopez, 2006.

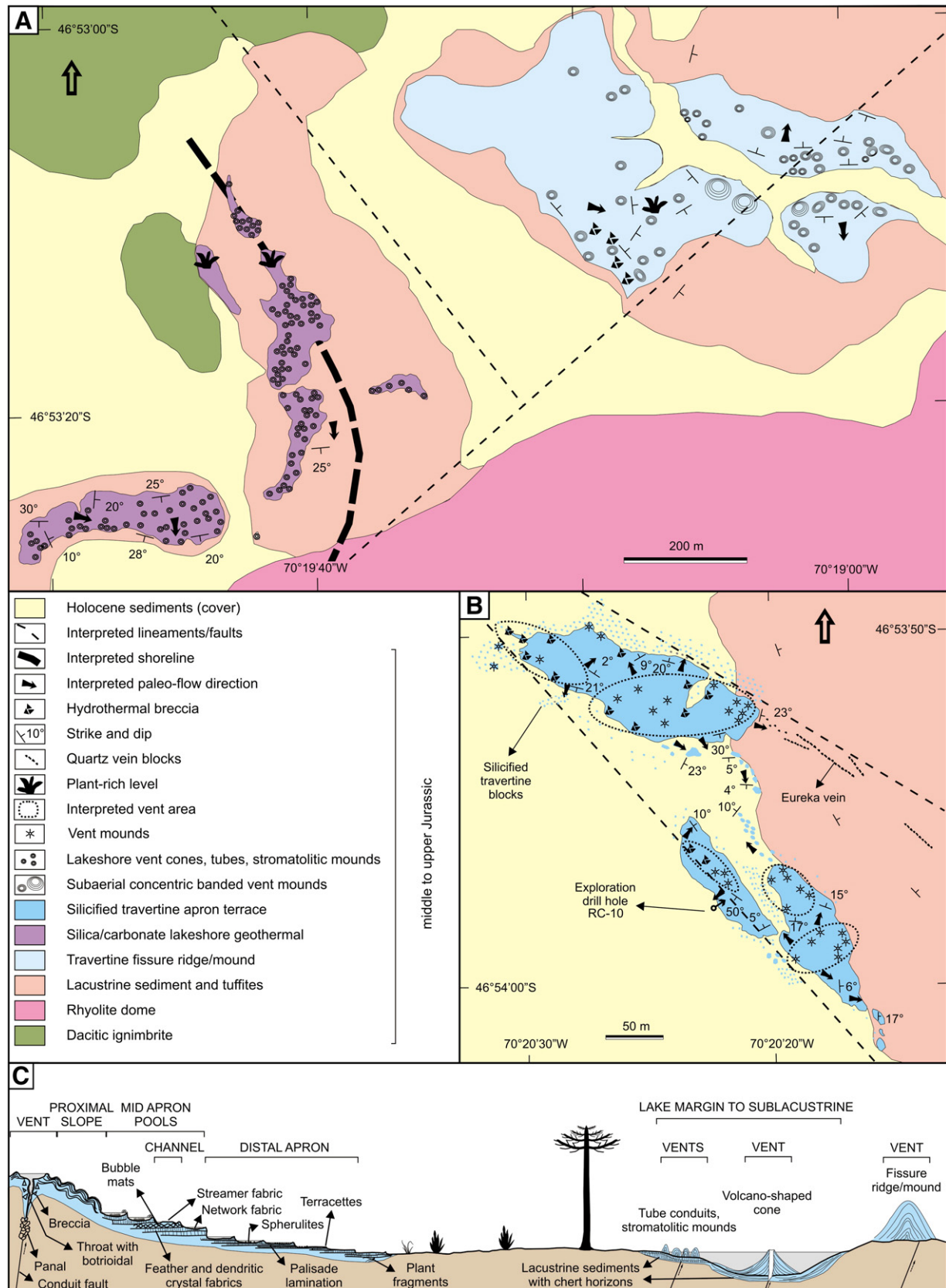


Fig. 2. Detailed geological maps for the Central (A) and Southwest (B) study areas shown in Fig. 1B. Thick black arrows indicate inferred hot spring-discharge (surface paleo-fluid flow) directions. In (A), an interpreted paleo-shoreline is indicated by the black thick dashed line. An inferred NE–SW fault separates a rhyolitic dome from the hot spring deposits ringing its northwestern border. An inferred NW–SE fault offsets the eastern Central area geothermal outcrops from the western Central area geothermal outcrops. (C) Schematic cross-section of geothermal paleoenvironments, based on facies identified in the Upper Jurassic deposits of the Cerro Negro geothermal area. Panel C is modified from Guido and Campbell, 2011.

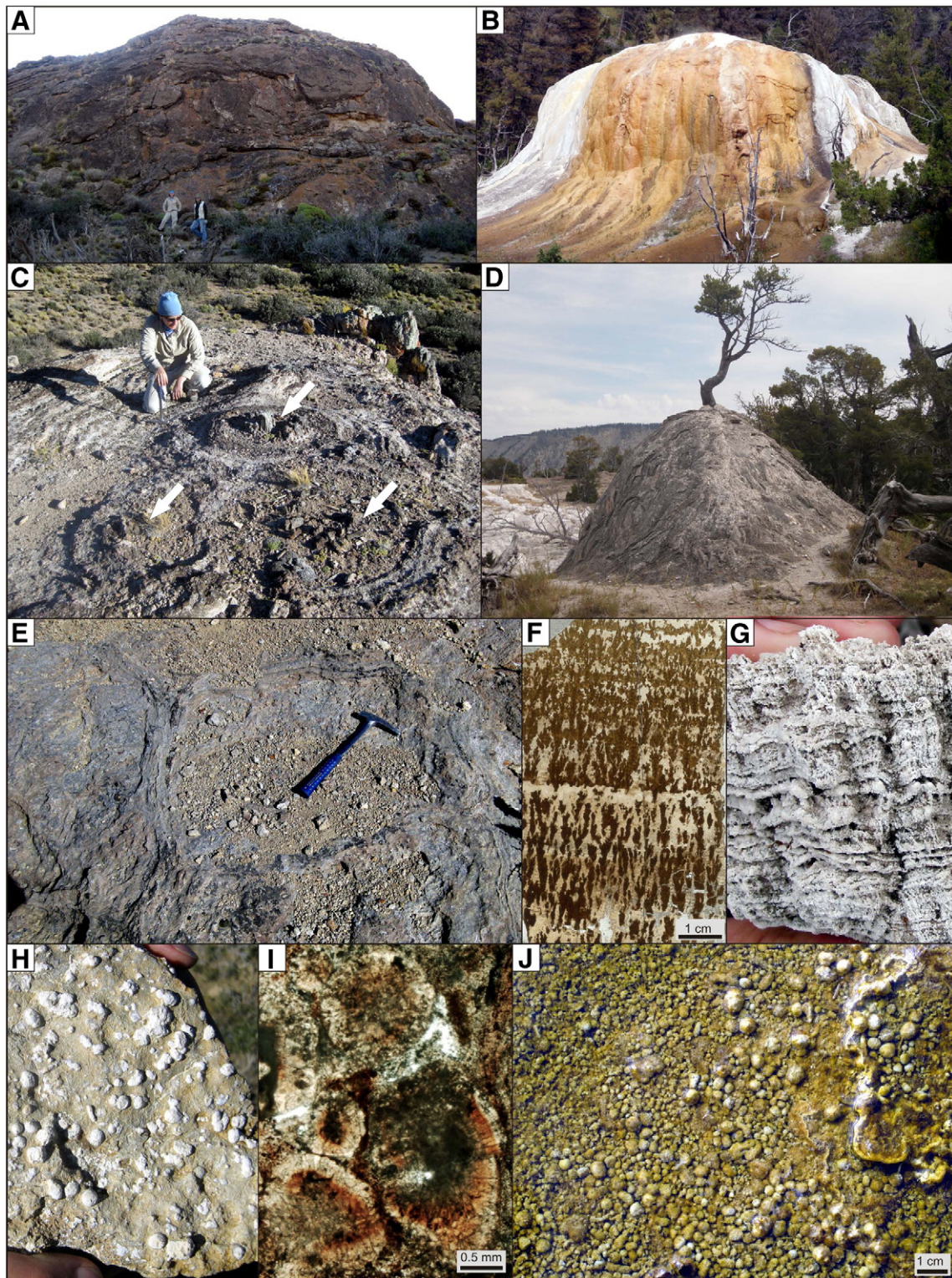


Fig. 3. Subaerial travertine fissure ridge/mound facies assemblages from the eastern part of the Central study area (Fig. 2A) at Cerro Negro, and comparison with facies and fabrics from Pleistocene–Recent deposits at Mammoth Hot Springs, Yellowstone National Park, U.S.A. (A) Large travertine mound from Cerro Negro, of comparable size and shape with (B) actively forming Orange Spring Mound, Yellowstone. (C) Travertine fissure mound (oblique view) at Cerro Negro showing decimeter-scale, concentric fabric that grew around three tree stumps (white arrows), compared with (D) travertine mound with a growing tree in the center, Yellowstone. (E) Giant scale panel structure affiliated with a large Cerro Negro fissure mound. (F) Dendritic travertine microtexture (entire thin section view, plane polarized light) from Cerro Negro, compared with (G) hand sample from inactive Mammoth Springs travertine, Yellowstone. (H) Hand sample and (I) thin section of Cerro Negro travertine with spherulitic texture, compared with (J) active Minerva Terrace at Mammoth Hot Springs, Yellowstone.

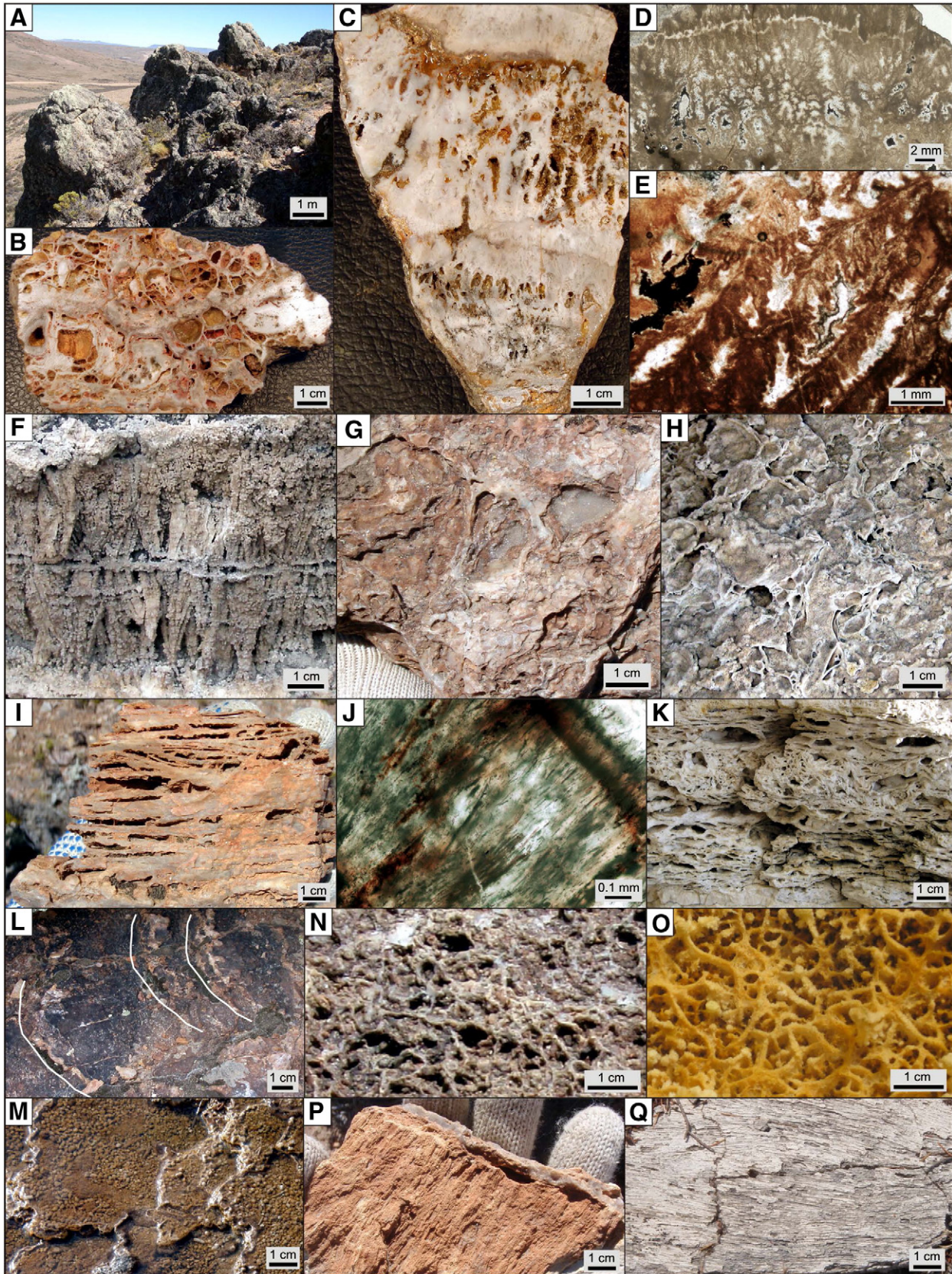
replaced travertine apron terrace facies (Fig. 4). Two additional, originally calcareous (now silica-replaced) deposit types include vent-conduit tube and stromatolitic mound facies (Fig. 5), interpreted

to have developed in wet lake margin/shoreline settings. A final deposit type is sublacustrine, comprising volcano-shaped cones that appear to have had a mixed silica–carbonate depositional/diagenetic

history (Fig. 6). These five hot spring-related facies types are described in detail in this section, while their paleoenvironmental relationships, inferred paleohydrologic signatures, and depositional/diagenetic histories are discussed further in Section 3.

2.2.1. Subaerial travertine fissure ridge/mound facies

We mapped 45 small to large (to 10 m high \times 40 m wide), round-topped, in places elongated, travertine ridge/mound features in the eastern part of the Central study area (Figs. 1B, 2A, 2C, 3). They are



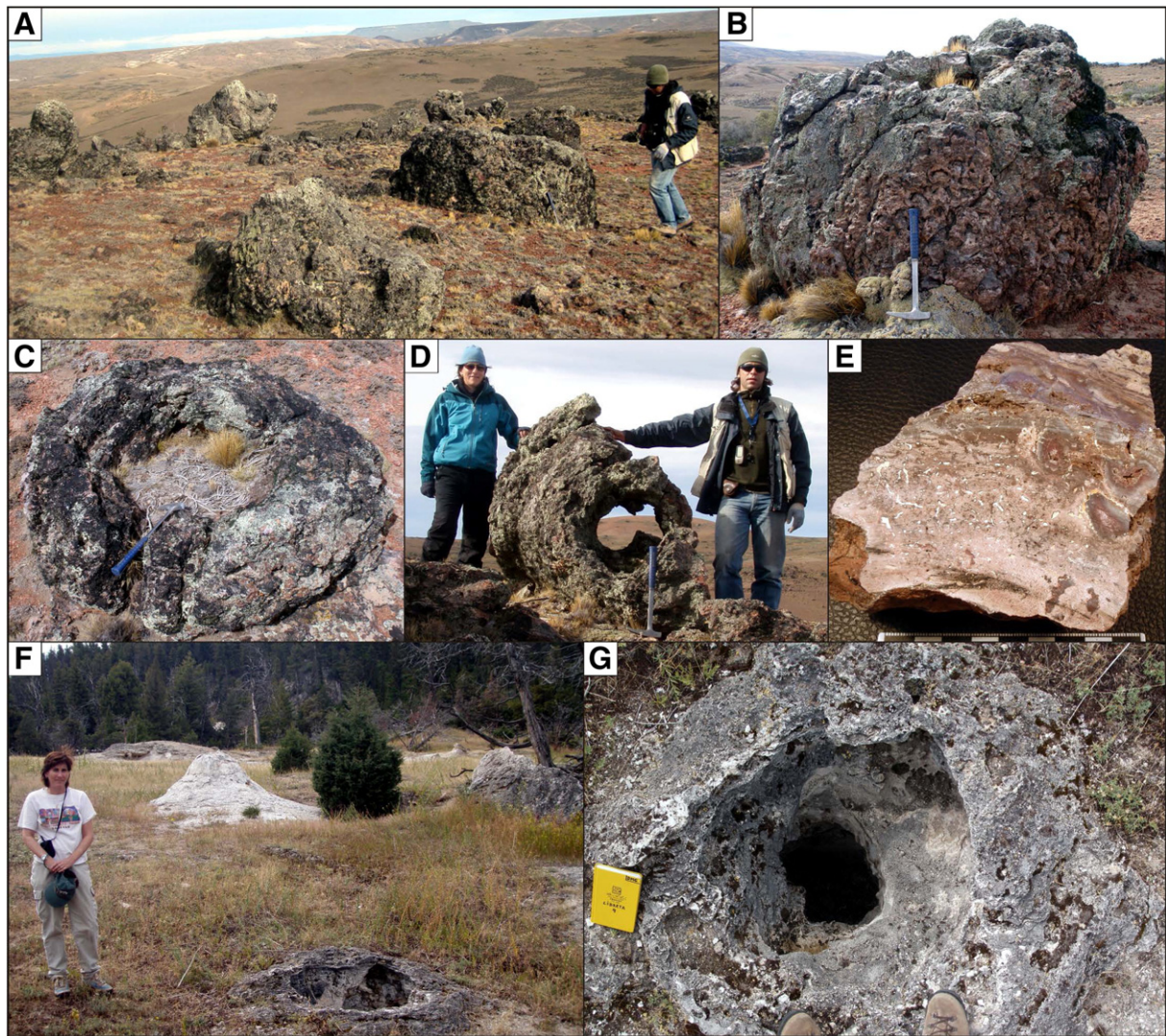


Fig. 5. Silica-replaced stromatolitic mound and siliceous vent-conduit tube facies, interpreted to have developed at wet lake margin/shoreline lake terrace settings, from the western outcrops of the Central area at Cerro Negro (Fig. 2A), and comparison with active and inactive geothermal deposits, southwestern area of Mammoth Hot Springs, Yellowstone National Park, U.S.A. (A, B, C) Stromatolitic vent mounds from Cerro Negro. (D) Travertine cylindrical vent-conduit tube, toppled and lying horizontally, Cerro Negro. (E) Thinly bedded lacustrine hand sample with chert horizons/nodules (upper) and silicified paleosol layer (lower), Cerro Negro. (F, G) Comparative examples of travertine mound (background) and vertically oriented vent-conduit tube (foreground, largely still in the ground), Yellowstone.

predominantly calcareous in composition, and compared closely in size and shape to travertine fissure-related ridges and mounds forming today at Mammoth Hot Springs in Yellowstone (Fig. 3A–B), and elsewhere. In travertine fissure systems, Hancock et al. (1999) suggested that mound morphologies occur where fissures are overlain by soft sediments; whereas, fissure ridges tend to develop where faults/fractures continue up to the surface. Five of the Cerro Negro mounds in this part of the study area contain one or more upright tree stumps (Fig. 3C), around which decimeter-scale, concentric travertine bands accumulated to build up the positive-relief features. At Mammoth Hot Springs today, trees grow out of active and inactive

fissure ridges and mounds (e.g., Fig. 3D), and often are engulfed and die in life position along rapidly advancing (mineralizing) travertine ridges, mounds and apron fronts. Internal exposures of the Cerro Negro fissure mounds contain siliceous panal structures (from “panal de abejas,” meaning beehive in Spanish), previously observed and interpreted to represent shallow, subterranean, tortuous, geothermal fluid flow pathways situated just beneath focused, surface vent emission areas (Guido and Campbell, 2011, Fig. 4F, p. 42). Some of the larger Cerro Negro fissure features contain giant panal structures (Fig. 3E). Another potential fossil panal example may be found in the silica–carbonate, medial fissure fill of the Late Pleistocene Ngakoringora

Fig. 4. Silica-replaced travertine apron terrace facies assemblages from the Southwest study area (Fig. 2B) at Cerro Negro, and comparison with similar features found in the Mammoth Hot Springs area, Yellowstone National Park, U.S.A. (A) Three deeply weathered vent mounds, Cerro Negro. (B) Panal texture associated with Cerro Negro vent mounds. (C) Hand sample and (D, E) thin section images (vertical sections) of “feather” crystal fabrics from Cerro Negro, compared with (F) outcrop (vertical section) from an inactive terrace, Yellowstone. (G) Bedding plane surface and (I) vertical section of Cerro Negro hand samples of wavy-laminated fabric with lenticular fossilized degassing bubbles, and a photomicrograph detail of fossilized (J) microbial filaments, compared with Hoodoo area (~300 ka) travertine textures at Yellowstone — (H) bedding plane surface and (K) vertical cross-section. (L) Arcuate micro-terracette feature from Cerro Negro (thin white lines outline low terracette lips), compared with (M) active travertine terracettes at Minerva Terrace, Yellowstone. (N) Network texture (bedding plane views) from Cerro Negro, compared with (O) modern example at Minerva Terrace, Yellowstone. (P) Bedding plane views of streamer fabric from Cerro Negro, compared with (Q) young fossilized example from inactive spring, Yellowstone.

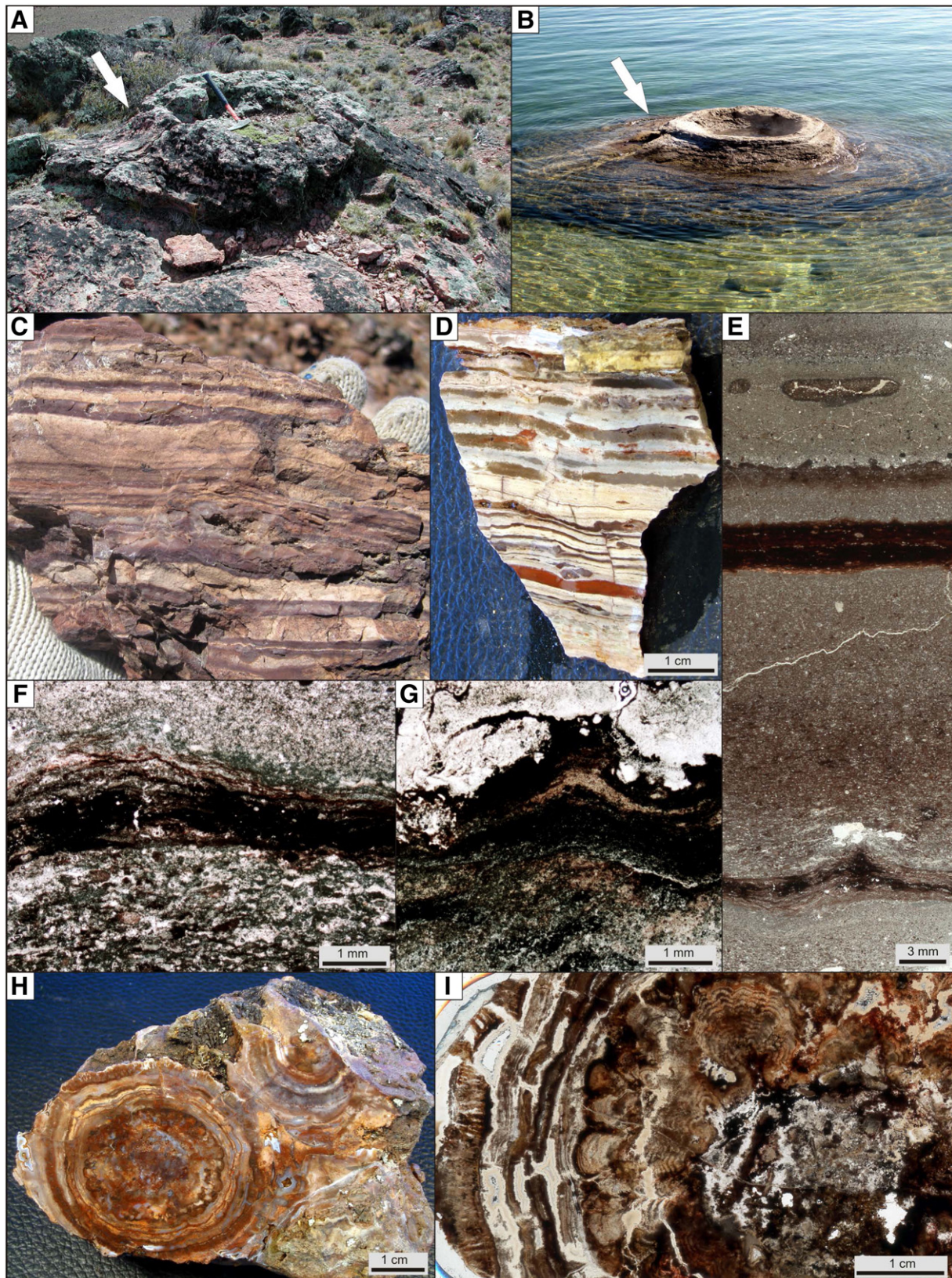


Fig. 6. Volcano-shaped cones and mixed silica-carbonate deposits in sublacustrine hot spring facies association from the westernmost outcrops of the Central area at Cerro Negro (Fig. 2A), and comparison with West Thumb area, Yellowstone National Park, U.S.A. (A) Volcano-shaped cone from Cerro Negro, compared with (B) steaming West Thumb example. Note the change in slope at flat lip of the exposed mouth of the vents (white arrows). (C–G) Thinly bedded lacustrine strata associated with fossil vent features of the volcano-shaped cones, showing interbedded chert horizons. Note the preserved fine laminae, crenulations and tufted structures, suggesting a microbial origin. (H, I) Silica-replaced, botryoidal stromatolites found at the bases of many cone features, or in clusters within lacustrine strata marginal to the vent field.

Ridge travertine fissure ridge/mound deposit in Kenya (cf. Renaut et al., 2002a, Fig. 4, p. 128), although preservation is poor at that locality.

Two relatively common carbonate textures associated with the Cerro Negro travertine fissure ridge/mound deposits include dendritic shrub (Fig. 3F) and spherulitic (Fig. 3H–I) fabrics, which also are found in Holocene (~8 kyr to modern; Sturchio et al., 1994) travertines of Yellowstone (Fig. 3G and 3J, respectively), and in Late Holocene and present-day fissure ridge travertines of Terme San Giovanni, Italy (Guo and Riding, 1994, Figs. 3, 4F, 11A). In addition, Cerro Negro dendritic fabrics are petrographically similar to dendritic aragonite needle shrubs forming today in warm pond facies at Angel Terrace, Mammoth Hot Springs (cf. Fig. 3F with Fig. 8E of Fouke et al., 2000, p. 574), and in Pleistocene thermal spring deposits of Cuatros Cienegas, Mexico (cf. plate 6C, Pentecost, 2005, p. 397). The dense, dark fabric of the dendrites in the Mexican travertine is attributed to dark bacterial inclusions in fibrous calcite crystals (Pentecost, 2005). Calcite spherules at Angel Terrace, analogous to Cerro Negro examples, form in the relatively cool distal slope facies described in Fouke et al. (2000). Similar, poorly preserved spherulites are reported from distal microterraces affiliated with Kenyan fossil travertine (Renaut et al., 2002a, Fig. 6E, p. 131). Small areas of plant-rich horizons also are found in spatially limited patches of the Cerro Negro fissure ridge/mound deposits, but here and in other parts of the study area (Fig. 2A), the plant stems are broken and appear to have been locally transported. Many are coated with thick stromatolitic growths (e.g., Fig. 6E, Guido and Campbell, 2011, p. 44) or microbial linings, indicating final deposition in wet and low areas.

2.2.2. Subaerial travertine apron terrace facies

Hot spring apron terraces with scattered vent mounds are exposed in the Southwest area of the study site (Figs. 1B, 2B–C, 4). They appear to comprise siliceous sinter and did form, in fact, in direct spatial association with the shallow epithermal Eureka siliceous (now quartz) vein system (Section 2.1; Figs. 1B, 2B). Nonetheless, textural and petrographic analysis verifies the Southwest area terraces as silica-replaced travertine in origin, described further below. The Southwest area also contains 32 mapped vent mounds (~2 m high × 3 m wide, e.g. Fig. 4A) in five main vent areas (Fig. 2B) based on outcrop morphology, rock texture and bedding dip directions. The vent mounds themselves are deeply weathered (Fig. 4A), with poorly preserved, irregular holes/pipes (probable conduits) riddling some mounds, and faint microbotrioids(?) rarely found on a few mound surfaces. Typical panel structures (Guido and Campbell, 2011) occur in basal and internal portions of many of the mounds (Fig. 4B), and several contain or were built upon hydrothermal/intraformational breccias.

Spatially associated with the poorly preserved vent mounds are blocky terraced outcrops (e.g., mapped deposits near exploration drill hole RC-10, Fig. 2B), which contain well-preserved fabrics typical of and similar to those reported from travertine apron terraces at Yellowstone and elsewhere (e.g., Chafetz and Folk, 1984; Fouke et al., 2000). As shown by Chafetz and Folk (1984), who compared Pleistocene travertine in Italy with actively forming travertine at Mammoth Hot Springs in Yellowstone, the facies associations are recurring and typically are spatially associated with microbes having different environmental distributions, and therefore producing different textural types (e.g., dendritic shrub, “feather” crystal). For example, feather fabrics (Figs. 4C–E) are well-preserved at Cerro Negro, and are akin to similar microtextures found on inactive and active terraces around the Mammoth area (Fig. 4F, cf. Fig. 4E with Fig. 9E of Fouke et al., 2000, p. 575). Fouke et al. (2000) sampled equivalent modern calcite feather crystal fabrics from microterraces in distal-slope facies at Angel Terrace. Pentecost (2005, plate 5D–E, p. 395) also illustrated analogous branching, feather crystal fabrics from present-day thermogene travertines in Italy

and Turkey. There is an ongoing debate regarding the abiotic versus biotic origin of dendritic shrub (e.g., Fig. 3F) and feather/ray crystal microfabrics (e.g., Fig. 4D–E) that also are common in many Pleistocene–Recent travertine apron and fissure ridge deposits (Chafetz and Folk, 1984; Pentecost, 1990; Guo and Riding, 1994; Fouke et al., 2000; Andrews and Riding, 2001; Fouke, 2001). In fact, Pentecost (2005) noted that clear distinctions between dendritic feather and shrub crystals are not always evident, and Chafetz and Guidry (1999) found a continuum between the two fabric types, arguing for a combination of biotic and abiotic processes in their formation (cf. Figs. 3F, 4E with Chafetz and Guidry, 1999, Fig. 2, p. 60).

The apron terraces of the Southwest study area at Cerro Negro contain additional paleoenvironmentally significant textures which correlate to Yellowstone and other thermogene travertines, such as wavy-laminated fabrics with large, curved lenticular voids (“bubble” mats with fossilized microbial filaments, Fig. 4G–K). Chafetz and Guidry (2003) illustrated similar features in Holocene travertine core from Mammoth, noting elongated, open pores parallel to bedding (their Fig. 6B, p. 1523) which indicate photosynthetic outgassing from microbial mats in hot spring channels and shallow pools (e.g., Hinman and Lindstrom, 1996; Pentecost, 2005). Arcuate micro-terrace features on bedding planes also are preserved in inferred distal apron settings at Cerro Negro, similar to Yellowstone examples (Fig. 4L–M). Analogous features are seen forming at Angel Terrace in Mammoth Hot Springs (cf. Fouke et al., 2000, Fig. 4F, p. 570), and are reported from Late Pleistocene thermogene travertine in Kenya (Renaut et al., 2002a, Fig. 2E–F). Some bedding planes at Cerro Negro preserve a ridged network texture, similar to Yellowstone examples (Fig. 4N–O), which represents calcified microbial filaments and their exopolymeric substances, or EPS. This fabric forms in moderate temperature spring pools and pool margins, such as at Angel Terrace (cf. Fouke et al., 2000, Fig. 4D, p. 570). Finally, the Southwestern area at Cerro Negro also contains some bedding plane surfaces with streamer fabric, representing carbonate-coated microbial “strings” typical of fast-flowing thermal outflows at Mammoth (Fig. 4P–Q), and elsewhere (Chafetz and Folk, 1984).

The western portion of the Central study area (Figs. 1B, 2A, C) comprises numerous small deposits of positive relief in three facies associations, representing mineralizing point-sources of geothermal fluid upflow in wet lake margin/shoreline to shallow sublacustrine paleoenvironments (Figs. 5, 6; and discussed further in Section 3). We mapped a N–S oriented field (Fig. 2A) of 80 stromatolitic mounds (~1.5 m high × 1–2 m diameter) and cylindrical vent-conduit tubes (~25 cm hole diameter × up to 2 m long; cf. Guido et al., 2002), the latter of which constitute botrioidal, concentric bands of silica-replaced carbonate (Fig. 5A–D). The deposits are associated with variably and thinly bedded, lacustrine strata with thin chert horizons/nodules that contain desiccation cracks, rip-up clasts and paleosol horizons (e.g., Fig. 5E). In the southwestern area of Mammoth Hot Springs today, subaerial fields of Subrecent carbonate mounds and hollow vent-tubes (Fig. 5F–G) serve as a somewhat analogous comparator for the Cerro Negro examples, as they are also numerous, of the same scale, and share some similar morphologies. However, the Cerro Negro vent deposits likely formed in a lake margin setting that alternated between wet and dry conditions, as evidenced by the abundance of cauliflower-shaped stromatolites constituting the mounds, and affiliation of the vent mounds and tubes with lake sediments that record desiccation events, soil development, and rolled (transported) partially indurated siliceous layers.

The fifth type of hot spring-related facies at Cerro Negro is found in the westernmost portion of the Central study area (Lopez et al., 2003), in an E–W oriented field (Figs. 1B, 2A, 2C) where 40 vents constituting stromatolitic mounds and also siliceous, volcano-shaped cones (~2 m high × 6 m wide; Fig. 6A) together are preserved in thinly to evenly bedded lacustrine strata with chert horizons/nodules. The volcano-shaped cones are abundant in the westernmost part of the

field area (Lopez et al., 2003). Some well-preserved cone examples show steepened lips, which are flat-topped and doughnut-shaped with a central hole, identical in size and shape with siliceous vent cones forming today along the shores of Yellowstone Lake at West Thumb (Fig. 6B). The upper portions of Cerro Negro cone textures comprise alternations of thinly bedded, lacustrine siltstone and chert horizons (Fig. 6C–E). Lopez et al. (2003, their Fig. 3) depicted a schematic stratigraphic section through two cone structures, illustrating brecciated central conduit portions filled with clasts of both stromatolites and laminated strata of irregular porosity (i.e. lacustrine siltstone/chert alternations). The laminated to thinly bedded to nodular chert horizons (Fig. 6D–G), reveal fine laminae to crenulations and, in places, preserve tufted structures suggestive of microbial origins (cf. Renaut et al., 2002b, Fig. 4, p. 242). The bases of many of these cones are surrounded by bulbous to cauliflower shaped, in situ stromatolitic “growths” of silica-replaced carbonate (Fig. 6H–I). Individual concentrations of these stromatolite aggregates also are found scattered within lacustrine strata on the margins of the cone field, inferred as distal/diffuse spring-influenced areas.

3. Discussion and conclusions

Because of the fortuitous burial–erosion history of Late Jurassic epithermal deposits throughout the Deseado Massif, exhumed fossil geothermal landscapes are largely intact and relatively common (e.g., Guido and Campbell, 2009; Guido et al., 2010; Guido and Campbell, 2011). Cerro Negro, in particular, affords an excellent opportunity to evaluate varied paleohydrologic signatures and paleoenvironmental transitions from subaerial to sublacustrine hydrothermally influenced settings (Section 3.1). Moreover, the diverse expressions of geothermal signals in sedimentary deposits of different composition (calcareous, siliceous) and diagenetic state (e.g., still calcareous vs. silicified travertines, termed “pseudosinters” herein) also can be evaluated with respect to depositional and post-depositional history (Section 3.2). The implications of our findings for a better understanding of preservation of microfacies and microbial fabrics in extreme environments are discussed further below.

3.1. Subaerial to sublacustrine paleoenvironments in the Cerro Negro geothermal system

Two striking aspects of the fossil geothermal system at Cerro Negro are the well-exposed spatial relationships evident among the five different hot spring subenvironments (Figs. 1B, 2), and their clearly expressed (morphological, textural, petrographic) transitions from subaerial to sublacustrine settings (Figs. 3–6). For example, the northeastern and southwestern limits of the study area (Fig. 1B) preserve subaerial travertine settings, specifically fissure ridge/mound and apron terrace subenvironments, respectively. In modern thermogene travertine environments, fissure ridges/mounds are typified by low rates of surface geothermal fluid outflow in comparison to apron terrace/pond settings (Fouke, 2001). Indeed, at Cerro Negro, we found more textural evidence for and variety of shallow subaqueous outflow in apron terrace deposits as compared to the fissure-related deposits (Figs. 3, 4). However, differences in timing and style of diagenesis for these two subaerial travertine deposit types also likely played a role in quality and extent of preservation of paleoenvironmentally significant fabrics (see Section 3.2 for further discussion).

In addition to the dry subaerial vs. wet subaerial differentiation in calcareous hot spring-deposit expression at Cerro Negro, the Central study area also preserves a northeast to southwest shift in adjacent geothermal-related settings, from fissure ridge/mound subaerial to alternating wet/dry lake margin/shoreline to shallow sublacustrine lake terrace paleoenvironments (Figs. 2A, C). For instance, remarkable similarities (size, shape, amount, composition) exist between the

Jurassic vent-tube conduits and Subrecent, subaerial Yellowstone examples (Fig. 5). We interpret the Cerro Negro tube conduits as the “throat” portions of subaerial to lake-shoreline vents. Within the same fossil vent field also occurs stromatolitic mounds, which show large-scale morphologies that appear to transition from the tube features (Fig. 5A–D). The stromatolitic mounds may represent continued, diffuse, mature-stage development of lake-margin fluid venting areas in perennially wet conditions. They are superficially similar to modern and fossil caddis fly-microbial bioherms found in lake sediments (geothermal, saline and freshwater related) in other parts of the world (Brues, 1927; Brown, 1948; Leggett and Cushman, 2001; Paik, 2005; Guido et al., 2010), but differ from the insect-microbial bioherms by their lack of fly larval cases, larger size, more irregular stromatolitic morphologies (cf. Fig. 5B–C with Fig. 1E of Guido et al., 2010, p. 12), and presence of irregular conduits.

Probably the most distinctive and unique fossil geothermal features at Cerro Negro are the volcano-shaped siliceous cones of the westernmost part of the Central study area (Figs. 2A, 6). The gross morphology and size of these deposits are identical with modern Yellowstone Lake vent cones, which are distributed along the shoreline and on the shallowly submerged lakeshore terrace at West Thumb, where many of the springs emit hot water and steam at present (Fig. 6B). Recent geophysical and submersible studies of Yellowstone Lake indicate more than 600 active and inactive hydrothermal vents, as well as submerged ancient shorelines, and a lake bottom topography controlled by a complex interplay of tectonics, volcanism, hydrothermal activity and glaciation (Morgan et al., 2003; 2007). On the Yellowstone lake bottom at various depths, several types of opaline silica deposits have been imaged, sampled, and analyzed including branching conduit tubes, ledges, domal structures, and “spires” that range from narrow and tall (1–2 m diameter × up to 8 m high) to conical (to 2 m high) at ~15 m water depths (Shanks et al., 2007; Morgan et al., 2007, Fig. 8A, p. 114). In Lake Taupo, New Zealand, siliceous hydrothermal conduits also have been described (Jones et al., 2007), but these small features display a chimney-type morphology not observed at Cerro Negro. Because of excellent three-dimensional exposure, the Cerro Negro vent cones can be investigated internally, with bases and interiors commonly consisting of intraformational breccias and broken or in situ stromatolites (Lopez et al., 2003), suggestive of shallow sublacustrine depositional conditions.

3.2. Distribution and preservation of Cerro Negro calcareous and siliceous hydrothermal deposits – depositional and diagenetic considerations

The Cerro Negro fossil geothermal system preserves an array of composition types, from carbonate to silica-replaced carbonate (pseudosinter) to siliceous deposits. Some vent fields, such as in the westernmost part of the Central study area, contain both siliceous (cone) and silica-replaced carbonate (stromatolite mound) fabrics in close spatial association. Here, we consider potential mechanisms for the original deposition of carbonate and/or silica under particular paleoenvironmental circumstances. Moreover, for certain deposits we evaluate possible syn/post-depositional (early or late diagenetic), differential silicification processes. Regionally, hot spring-associated faults likely delivered silicon or calcium carried in migrating hydrothermal fluids to surface discharge areas (Guido and Campbell, 2011). Widespread silica-hosted precious and base metal mineralization (Schalamuk et al., 1997) may have been derived from the extensive rhyolitic volcanics of the region. The origin of the carbonate in the travertines was likely from magmatic CO₂ degassing (e.g., Yoshimura et al., 2004; Pentecost, 2005; Gibert et al., 2009) because there is no significant source of carbonate in the Precambrian or Phanerozoic stratigraphy of the Deseado Massif (De Giusto et al., 1980).

The travertine fissure ridge/mound deposits in the eastern part of the Central study area (Figs. 2A, 3) are remarkably well-preserved

considering their Late Jurassic age, e.g. in comparison to Late Pleistocene travertine exposed in the Turkana Basin, Kenya (Renaut et al., 2002a). The Kenyan Ngakoringora Ridge is unlikely to have been buried since its probable Pleistocene age of formation, and yet has undergone relatively severe chemical and physical weathering (Renaut et al., 2002a). By contrast, the Cerro Negro fissure ridge/mound area likely formed in a paleo-valley and was buried by fine-grained sediments to be preserved in a relatively intact state.

The other subaerial travertine deposit at Cerro Negro, now silica replaced and exposed in the Southwestern study area (Figs. 2B, 4), shows two types of preservation states – poor (vent mounds) and excellent (apron terrace). The travertine is positioned directly upon the Eureka epithermal quartz vein–fault system, and we suggest the pristine preservation of many types of apron terrace fabrics can be attributed to both the inferred wet (pond, channel) conditions and early silicification of the terraces, forming pseudosinter along the fault. The poor preservation of fabrics in the vent mounds may indicate rapid diagenetic modification of metastable, high-temperature vent carbonates (e.g., neomorphism of acicular aragonite microfabrics that may have constituted the microbotrioids), and/or long-term subaerial exposure/weathering (cf. Kenyan Ngakoringora Ridge), owing to their stratigraphic position at the top of the apron sequence. In distal apron subenvironments in the Southwestern study area, fossil microbial filaments show excellent preservation (Fig. 4J), similar to the inferred paleo-settings for exceptional plant, microbe and arthropod preservation found in the San Agustín sinter of the Deseado Massif (Guido et al., 2010) and in the Devonian Rhynie Chert of Scotland (e.g., Trewin et al., 2003). It is noteworthy that the Southwestern area travertine at Cerro Negro shows such promise for additional detailed geobiological study because elsewhere in the Deseado Massif what now constitute pseudosinter deposits typically experienced intense physical and chemical weathering prior to late-stage hydrothermal silicification (Guido and Campbell, personal observations).

The lake margin/shoreline and shallow sublacustrine platform vents (Figs. 5, 6; tube-conduits, stromatolitic mounds, volcano-shaped cones) of the western part of the Central study area (Fig. 2A) show broad morphologic similarities with both travertine and sublacustrine sinters from Yellowstone (e.g., inactive geothermal areas at Mammoth Hot Springs and along Yellowstone Lake at West Thumb). The three vent facies types at Cerro Negro are spatially affiliated with lacustrine strata containing chert bands and nodules that we infer as hydrothermal in origin (see below), thus serving as the likely source of silica replacing the carbonates in this mixed silica–carbonate system.

The abundant chert bands and nodules evident in the lake-associated deposits positioned close to fossil vents/mounds at Cerro Negro have at least two explanations as to their potential formation mechanism(s), as discussed here in relation to potentially analogous, Late Pleistocene, geothermally influenced siliceous deposits from the Baringo and Magadi lake areas in Kenya (Behr and Röhrlich, 2000; Renaut et al., 2002b). The Cerro Negro examples are somewhat similar in texture to sublacustrine sinter described from Lake Baringo, in that both show laminated to massive, crustose to pore-filling fabrics that formed in affiliation with lake-floor hot springs (Renaut and Owen, 1988; Renaut et al., 2002b). Renaut et al. (2002b) suggested an origin of the Baringo silica from a deep, hot alkali chloride reservoir, discharging via lake-floor springs, with silica gel accumulating on the lake bottom or within shallow (<1 m) sediments infused with thermal fluids. Complete mixing of the spring and lake water was likely retarded in some manner (e.g., interstitial precipitation, or within diatom-microbial mats) so that amorphous silica saturation would have been reached locally as the fluid temperatures dropped, fluid composition changed or evapo-transpiration increased (e.g., Renaut et al., 1998; Renaut et al., 1999; Renaut et al., 2002b). In this case, the chert layering would have been caused by intervals of more vigorous

geothermal discharge, and/or change in temperature, pH, salinity, or fluid composition. At Lake Magadi, Behr and Röhrlich (2000) demonstrated the ultimate origin of most Magadi-type chert bands from within growth layers of carbonate-secreting cyanobacteria. The ensuing, microbially formed crusts and other originally calcareous deposits underwent syn-depositional or early post-depositional silicification within mat-coated, lakeshore mudflat and solar heated pond settings. Evapotranspiration and reaction of warm spring and/or alkaline lake waters with volcanoclastic sediments are inferred to have increased pH locally to produce viscous silica sols and gels that replaced the carbonate in the microbial mats. Rhythmicity of chert horizons in these deposits was attributed to pH variation under biochemical (microbial) control (Behr and Röhrlich, 2000). From this first broad assessment of Cerro Negro geothermally influenced deposits, it is not possible to determine with certainty the source of the chert bands in the lake-affiliated strata of the fossil vent areas, and their possible hydrothermal origin needs to be investigated in more detail in the future.

3.3. Overall summary and significance of Cerro Negro epithermal system

Collectively the presence of porphyritic intrusions, deeper exposures of low sulfidation epithermal veins (i.e., Eureka northwest segment described in Lopez, 2006, and Au- and Ag-rich veins – Eureka West, San Marcos, Mariana Norte and Mariana Central – outlined in Shatwell et al., 2011), and the differential geographic distribution of surface hot spring occurrences across the study site are all in agreement with the hypothesis that the NW volcanic emission center exposes relatively deeper levels of the Cerro Negro epithermal system than the SE emission center. Therefore, a general deepening level of exposure can be inferred from SE to NW. The regional faults between the two interpreted emission centers host the epithermal mineralization, but the western and eastern faults appear to contain higher grade veins closer to the NW emission center. Moreover, the western fault associated with the Eureka vein also allowed early silicification of the travertine deposits at the paleo-surface in the SE emission center.

The diverse facies associations and excellent paleogeographic exposure of the Cerro Negro geothermal system illustrate paleo-spring fluid flow directions (Fig. 2A–B) and shifting paleohydrologic conditions in which hot spring deposits developed and interacted in different ways with their surrounding depositional (sedimentary) environments. Specifically Cerro Negro archives a well-preserved record of subaerial, thermogene travertine apron terraces and fissure ridge/mound settings representing high- to low-rates of fluid discharge, as well as lake-related, wet shoreline to sublacustrine vent-deposit transitions. Microbial fabrics and stromatolites are common constituents of most Cerro Negro geothermal subenvironments. We found a diversity of rock types among the geothermal deposits, including those formed from precipitating and/or diagenetic fluids of carbonate, silica or mixed silica–carbonate composition.

Early silicification of travertine aprons to produce pseudosinter along the Eureka fault, which also hosts a prominent and extensive quartz vein outcrop, suggests a direct link between the shallow epithermal and surface geothermal portions of the Cerro Negro hydrothermal system. In this particular area, silica-replaced, apron-terrace microbial fabrics are well-preserved, and imply that narrowing the search for Lagerstätten-style conditions in these types of extreme paleoenvironments should take into consideration geologic context and syn-/post-depositional history to identify similar deposits of potentially excellent preservation in the geological record.

Acknowledgments

We acknowledge the National Geographic Society, CONICET, La Plata University, the Royal Society of New Zealand's Charles Fleming Senior Scientist Fund, the INREMI (Instituto de Recursos Minerales),

and the University of Auckland's Faculty Research Development Fund for financial and other support of this project. We also thank Andean Resources for allowing access to the field area. We acknowledge Alan Channing and Alba Zamuner for their participation during the first stage of the field observations. Nancy Hinman and Jack Farmer provided fruitful discussions and logistical support at Yellowstone, and Priscilla Cameron aided us in obtaining literature references, for which we are most grateful. Robin Renaut and an anonymous reviewer provided comments that improved the quality of the manuscript.

References

- Andrews, J.E., Riding, R., 2001. Depositional facies and aqueous-solid geochemistry of travertine-depositing hot springs (Angel Terrace, Mammoth Hot Springs, Yellowstone National Park, U.S.A.)—Discussion. *Journal of Sedimentary Research* 71, 496–497.
- Behr, H.-J., Röhrlich, C., 2000. Record of seismotectonic events in siliceous cyanobacterial sediments (Magadi cherts), Magadi Lake, Kenya. *International Journal of Earth Sciences* 89, 268–283.
- Brown, R.W., 1948. Algal pillars miscalled geyser cones. June Annual Report of the Board of Regents of the Smithsonian Institution, pp. 277–290.
- Brues, C.T., 1927. Animal life in hot springs. *The Quarterly Review of Biology* 2, 181–203.
- Chafetz, H.S., Folk, R.L., 1984. Travertines: depositional morphology and the bacterially constructed constituents. *Journal of Sedimentary Petrography* 54, 289–316.
- Chafetz, H.S., Guidry, S.A., 1999. Bacterial shrubs, crystal shrubs, and ray-crystal shrubs: bacterial vs. abiotic precipitation. *Sedimentary Geology* 126, 57–74.
- Chafetz, H.S., Guidry, S.A., 2003. Deposition and diagenesis of Mammoth Hot Springs travertine, Yellowstone National Park, Wyoming, U.S.A. *Canadian Journal of Earth Sciences* 40, 1515–1529.
- Channing, A., Zamuner, A., Edwards, D., Guido, D., 2011. *Equisetum thermale* sp. nov. (Equisetales) from the Jurassic San Agustín hot spring deposit, Patagonia: anatomy, paleoecology and inferred paleoecophysiology. *American Journal of Botany* 98, 680–697.
- De Giusto, J., Di Persia, A., Pezzi, E., 1980. El Nesocratón del Deseado. II Simposio de Geología Regional Argentina, Tomo 2. Academia Nacional Ciencias, Córdoba, pp. 1389–1430.
- Echeveste, H., Fernández, R., Bellieni, G., Tessone, M., Llambias, E., Schalamuk, I., Piccirillo, E., De Min, A., 2001. Relaciones entre las Formaciones Bajo Pobre y Chon Aike (Jurásico medio a superior) en el área de Estancia El Fénix-Cerro Huemul, zona centro-occidental del Macizo del Deseado, provincia de Santa Cruz. *Revista de la Asociación Geológica Argentina* 56 (4), 548–558.
- Fouke, B.W., 2001. Depositional facies and aqueous-solid geochemistry of travertine-depositing hot springs (Angel Terrace, Mammoth Hot Springs, Yellowstone National Park, U.S.A.)—reply. *Journal of Sedimentary Research* 71, 497–500.
- Fouke, B.W., Farmer, J.D., Des Marais, D.J., Pratt, L., Sturchio, N.C., Burns, P.C., Discipulo, M.K., 2000. Depositional facies and aqueous-solid geochemistry of travertine-depositing hot springs (Angel Terrace, Mammoth Hot Springs, Yellowstone National Park, U.S.A.). *Journal of Sedimentary Research* 70, 565–585.
- García Massini, J., Channing, A., Guido, D.M., Zamuner, A.B., 2012. First report of fungi and fungus-like organisms from Mesozoic hot springs. *Palaos* 27, 55–62.
- Giacosa, R., Zubia, M., Sánchez, M., Allard, J., 2010. Meso-Cenozoic tectonics of the southern Patagonian foreland: structural evolution and implications for Au–Ag veins in the eastern Deseado region (Santa Cruz, Argentina). *Journal of South American Earth Sciences* 30, 134–150.
- Gibert, R.O., Taberner, C., Sáez, A., Giral, S., Alonso, R.N., Edwards, R.L., Pueyo, J.J., 2009. Igneous origin of CO₂ in ancient and recent hot-spring waters and travertines from the northern Argentinean Andes. *Journal of Sedimentary Research* 79, 554–567.
- Guido, D., 2004. Subdivisión litofacial e interpretación del volcanismo jurásico (Grupo Bahía Laura) en el este del Macizo del Deseado, provincia de Santa Cruz. *Revista de la Asociación Geológica Argentina* 59 (4), 727–742.
- Guido, D.M., Campbell, K.A., 2009. Jurassic hot-spring activity in a fluvial setting at La Marciana, Patagonia, Argentina. *Geological Magazine* 146 (4), 617–622.
- Guido, D.M., Campbell, K.A., 2011. Jurassic hot spring deposits of the Deseado Massif (Patagonia, Argentina): characteristics and controls on regional distribution. *Journal of Volcanology and Geothermal Research* 203, 35–47.
- Guido, D., Schalamuk, I., 2003. In: Eliopoulos, D., et al. (Ed.), Genesis and exploration potential of epithermal deposits from the Deseado Massif, Argentinean Patagonia. Mineral Exploration and Sustainable Development, I. Balkema-Rotterdam, Holanda, pp. 489–492.
- Guido, D., Delupí, R., López, R., de Barrio, R., Schalamuk, I., 2002. Estromatolitos y mineralización epitermal en el área Marianas-Eureka. *Actas II Macizo del Deseado, Santa Cruz. XV Congreso Geológico Argentino, Calafate*, pp. 284–289.
- Guido, D., Escayola, M., de Barrio, R., Schalamuk, I., Franz, G., 2006. La Formación Bajo Pobre (Jurásico) en el este del Macizo del Deseado, Patagonia: Vinculación con el Grupo Bahía Laura. *Revista de la Asociación Geológica Argentina* 61 (2), 187–196.
- Guido, D.M., Channing, A., Campbell, K.A., Zamuner, A., 2010. Jurassic geothermal landscapes and fossil ecosystems at San Agustín, Patagonia, Argentina. *Journal of the Geological Society of London* 167, 11–20.
- Guo, L., Riding, R., 1994. Origin and diagenesis of Quaternary travertine shrub fabrics, Rapolano Terme, central Italy. *Sedimentology* 41, 499–520.
- Hancock, P.L., Chalmers, R.M.L., Altunel, E., Kahir, Z., 1999. 'Travitonics': using travertine in active fault studies. *Journal of Structural Geology* 21, 903–916.
- Hinman, N.W., Lindstrom, L.F., 1996. Seasonal changes in silica deposition in hot spring systems. *Chemical Geology* 132, 237–246.
- Jones, B., De Ronde, C.E.J., Renaut, R.W., Owen, R.B., 2007. Siliceous sublacustrine spring deposits around hydrothermal vents in Lake Taupo, New Zealand. *Journal of the Geological Society of London* 164, 227–242.
- Leggitt, V.L., Cushman Jr., R.A., 2001. Complex caddisfly-dominated bioherms from the Eocene Green River Formation. *Sedimentary Geology* 145, 377–396.
- Lopez, R.G., 2006. Estudio Geológico-Metalogénico del área oriental al curso medio del Río Pinturas, sector noroeste del Macizo del Deseado, provincia de Santa Cruz, Argentina. Unpublished PhD thesis, Universidad Nacional de La Plata, 226 p.
- Lopez, R., Guido, D., Schalamuk, I., de Barrio, R., 2003. Las Margaritas, un sinter jurásico vinculado a mineralización aurífera en el noroeste del Macizo del Deseado, provincia de Santa Cruz, Argentina., in X Congreso Geológico Chileno: Concepción, Chile, Universidad de Concepción. 9 p.
- Morgan, L.A., Shanks III, W.C., Lovalvo, D.A., Johnson, S.Y., Stephenson, W.J., Pierce, K.L., Harlan, S.S., Finn, C.A., Lee, G., Webring, M., Schulze, B., Dühn, J., Sweeney, R., Balistrieri, L., 2003. Exploration and discovery: results from high-resolution sonar imaging, seismic reflection profiling, and submersible studies. *Journal of Volcanology and Geothermal Research* 122, 221–242.
- Morgan, L.A., Shanks III, W.C., Pierce, K.L., Lovalvo, D.A., Lee, G.K., Webring, M.W., Stephenson, W.J., Johnson, S.Y., Harlan, S.S., Schulze, B., Finn, C.A., 2007. The floor of Yellowstone Lake is anything but quiet—new discoveries from high-resolution sonar imaging, seismic-reflection profiling, and submersible studies. In: Morgan, L.A. (Ed.), Integrated Geoscience Studies in the Greater Yellowstone Area—Volcanic, Tectonic, and Hydrothermal Processes in the Yellowstone Geoecosystem: U.S. Geological Survey Professional Paper 1717, pp. 95–126.
- Paik, I.S., 2005. The oldest record of microbial-caddisfly bioherms from the Early Cretaceous Jinju Formation, Korea: occurrence and palaeoenvironmental implications. *Palaeogeography, Palaeoclimatology, Palaeoecology* 218, 301–315.
- Pankhurst, R.J., Leat, P.T., Sruoga, P., Rapela, C.W., Marquez, M., Storey, B.C., Riley, T.R., 1998. The Chon Aike province of Patagonia and related rocks in West Antarctica: a silicic large igneous province. *Journal of Volcanology and Geothermal Research* 81, 113–136.
- Pentecost, A., 1990. The formation of travertine shrubs: Mammoth Hot Springs, Wyoming. *Geological Magazine* 127 (2), 159–168.
- Pentecost, A., 2005. Travertine. Springer, Berlin. 445 pp.
- Renaut, R.W., Owen, R.B., 1988. Opaline cherts associated with sublacustrine hydrothermal springs at Lake Bogoria, Kenya Rift valley. *Geology* 16 (8), 699–702.
- Renaut, R.W., Jones, B., Tiercelin, J.-J., 1998. Rapid in situ silicification of microbes at Loburu hot springs, Lake Bogoria, Kenya Rift Valley. *Sedimentology* 45, 1083–1103.
- Renaut, R.W., Jones, B., Le Turdu, C., 1999. Calcite lily pads and ledges at Lorusio Hot Springs, Kenya Rift Valley: travertine precipitation at the air–water interface. *Canadian Journal of Earth Sciences* 46, 649–666.
- Renaut, R.W., Jones, B., Tiercelin, J.-J., Tarits, C., 2002a. Sublacustrine precipitation of hydrothermal silica in rift lakes; evidence from Lake Baringo, central Kenya Rift valley. *Sedimentary Geology* 148, 235–257.
- Renaut, R.W., Morley, C.K., Jones, B., 2002b. Fossil hot-spring travertine in the Turkana basin, northern Kenya: structure, facies, and genesis. In: Renaut, R.W., Ashley, G.M. (Eds.), Sedimentation in Continental Rifts, SEPM Special Publication No. 73, pp. 123–141.
- Richardson, N.J., Underhill, J.R., 2002. Controls on the structural architecture and sedimentary character of syn-rift sequences, North Falkland Basin, South Atlantic. *Marine and Petroleum Geology* 19, 417–443.
- Schalamuk, I., Zubia, M., Genini, A., Fernández, R., 1997. Jurassic epithermal Au–Ag deposits of Patagonia, Argentina. *Ore Geology Reviews* 12 (3), 173–186.
- Shanks III, W.C., Alt, J.C., Morgan, L.A., 2007. Geochemistry of sublacustrine hydrothermal deposits in Yellowstone Lake—hydrothermal reactions, stable-isotope systematics, sinter deposition and spire formation. In: Morgan, L.A. (Ed.), Integrated Geoscience Studies in the Greater Yellowstone Area—Volcanic, Tectonic, and Hydrothermal Processes in the Yellowstone Geoecosystem: U.S. Geological Survey Professional Paper 1717, pp. 205–234.
- Shatwell, D., Clifford, J.A., Echavarría, D., Irusta, G., Lopez, D., 2011. (April) Discoveries of low-sulfidation epithermal Au–Ag veins at Cerro Negro, Deseado Massif, Argentina: SEG Newsletter, 85, pp. 16–23.
- Sturchio, N.C., Pierce, K.L., Murrell, M.T., Storey, M.L., 1994. Uranium-series ages of travertine and timing of the last glaciation in the northern Yellowstone area, Wyoming–Montana. *Quaternary Research* 41, 265–277.
- Trewin, N.H., Fayers, S.R., Kelman, R., 2003. Subaqueous silicification of the contents of small ponds in an Early Devonian hot-spring complex, Rhynie, Scotland. *Canadian Journal of Earth Sciences* 40, 1697–1712.
- Yoshimura, K., Liu, Z., Cao, J., Yuan, D., Inokura, Y., Noto, M., 2004. Deep source CO₂ in natural waters and its role in extensive tufa deposition in the Huanglong Ravines, Sichuan, China. *Chemical Geology* 205, 141–153.